A Two Step Post-Synthetic Modification Strategy: Appending Short Chain Polyamines to Zn-NH_2-BDC MOF for Enhanced CO_2 Adsorption

*Anita Justin, Jordi Espín, Ilia Kochetygov, Mehrdad Asgari, Olga Trukhina, Wendy Queen**

Institute of Chemical Sciences and Engineering, École Polytechnique Fédérale de Lausanne (EPFL), CH-1951 Sion, Switzerland

SUBJECTS: Metal-Organic Frameworks, Post-synthetic modification, IRMOF-3, amines, CO_2 capture.

ABSTRACT

Functionalizing metal-organic frameworks (MOFs) with amines is a commonly used strategy to enhance their performance in CO_2 capture applications. As such, in this work, a two-step strategy to covalently functionalize NH_2-containing MOFs with short chain polyamines was developed. In the first step, the parent MOF, $Zn_4O(NH_2\text{-}BDC)_3$, was exposed to bromoacetyl bromide (BrAcBr), which readily reacts with pendant -NH_2 groups on the 2-amino-1,4-benzenedicarboxylate (NH_2-BDC^{2-}) ligand. ^{1}H-NMR of the digested MOF sample revealed that as much as 90 % of the MOF ligands could be functionalized in the first step. Next, the MOF samples, having 60% of the ligands functionalized with acetyl bromide, $Zn_4O(NH_2\text{-}BDC)_{1.2}(BrAcNH\text{-}BDC)_{1.8}$, was exposed to several

short chain amines including ethylenediamine (ED), diethylenetriamine (DETA) and tris(2-aminoethyl) amine (TAEA). Subsequent digested ^{1}H-NMR analysis indicated that a total of 30 %, 28 % and 19 % of the MOF ligands were successfully grafted to ED, DETA and TAEA, respectively. Next, the CO_2 adsorption properties of the amine grafted MOFs were studied. The best performing material, TAEA-appended-$Zn_4O(NH_2\text{-BDC})_{1.2}(BrAcNH\text{-BDC})_{1.8}$, exhibits a zero-coverage isosteric heat of CO_2 adsorption of -62.5 kJ/mol, a value that is considerably higher than the one observed for the parent framework, -21 kJ/mol. Although the boosted CO_2 affinity only leads to a slight increase in the CO_2 adsorption capacity in the low-pressure regime (0.15 bar), which is of interest in post-combustion carbon dioxide capture, the CO_2/N_2 (15/85) selectivity at 313 K is 143, a value that is ~ 35 times higher than the one observed for $Zn_4O(NH_2\text{-BDC})_3$, 4.1. Such enhancements are attributed to accessible primary amines, which were grafted to the MOF ligand. This hypothesis was further supported via *in-situ* DRIFTS measurements of TAEA-Ac-$Zn_4O(NH_2\text{-BDC})_{1.2}(BrAcNH\text{-BDC})_{1.8}$ after exposure to CO_2, which revealed the chemisorption of CO_2 via the formation of hydrogen bonded carbamates/carbamic acid and $CO_2^{\delta-}$ species; the latter are adducts formed between CO_2 and $[amineH]^+Br^-$ salts that are produced during the amine grafting step.

Synopsis

Amines are covalently grafted to the $Zn_4O(NH_2\text{-BDC})_3$ (IRMOF-3) framework via a new, two-step post-synthetic modification strategy. The feasibility of the reaction is proved and the conversion in each step is quantitatively assessed. The CO_2 adsorption performance and mechanism are studied.

Introduction

Metal-organic frameworks (MOFs) are a unique class of crystalline materials that offer outstanding porosity, a high degree of structural tunability, and easy modular syntheses.[1] Due to these attractive features, the assessment of MOFs in various energy and ecologically relevant applications, such as gas storage and separation,[2-4] catalysis,[5] water treatment,[6] etc, is currently underway. Of the many potential functions, one might choose to engineer into MOF structures, ever growing CO_2 concentration and persistent increases in global temperatures has motivated the design of many new MOFs and MOF-based composites that can selectively extract CO_2 from gas mixtures, thereby promoting MOF deployment into carbon capture technologies. To date, there are a number of innovative strategies used to design MOFs for carbon capture including: i) the direct synthesis of MOFs having a variety of polarizing functionality on their internal surface creating strong electrostatic type interactions between the host framework and CO_2[7-9] and ii) the post-synthetic modification (PSM) of MOFs, with alkylamines that are either appended to open metal coordination sites (OMS)[10-12] or simply impregnated into the structure.[13-14] While the latter have yielded many amine-containing MOFs with high CO_2 capacity and selectivity, they sometimes fail to retain their CO_2 capacity in humid conditions where water molecules can eventually displace the metal-amine coordination bond with adsorption/desorption cycling; this leads to volatile amine species leaching from the MOF pores and a loss in performance.[15]

Recently, we have begun exploring other approaches to insert pendant amines into MOF pores. For instance, a less thoroughly explored PSM approach that might avoid amine loss and the resulting decline in CO_2 cycling capacity is to covalently graft the amines directly onto the MOF ligand. For example, in 2010, Yaghi et al. demonstrated the first amine grafting into IRMOF-3 via ring opening reaction of 2-methylazidirine.[16] After the PSM, proven via solid state ^{13}C-NMR, the resulting MOF was not assessed for CO_2 adsorption, despite a likely increase in the density of

primary amines. In 2018, Shojaei et al. grafted ethylenediamine (ED) onto the ligand in a MOF known as UiO-66-NH_2 via a Michael addition, using glycidyl methacrylate as a bridge between the MOF ligand and ED.[17] The aim of this study was to improve the CO_2/CH_4 selectivity at high pressures (20 bar) by introducing extra amine groups. Unfortunately, due to the small pore aperture of the selected MOF, the reaction occurred on the external MOF surface. Moreover, while the mechanism of CO_2 adsorption of the ED modified MOF was proposed, the authors did not give insight into enhancement in the CO_2 adsorption capacity at low pressures. Similarly, in 2019 Li et al. grafted polyethyleneimine (PEI) on UiO-66-NH_2 with glutaraldehyde as the bridging molecule, in order to enhance the CO_2 selectivity at 0.15 bar.[18] For this, PEI (MW= 600 g/mol) was grafted to the external and part of the internal surface of UiO-66-NH_2 increasing the CO_2/N_2 (15/85) selectivity from 25 to 48, albeit, the extent of amine grafting was not assessed. Given that the literature is limited to these few studies, much work is left to be done to fully understand how the extent of various grafting reactions and the amine structure impact the performance of diverse MOFs in CO_2 separations. Unfortunately, unlike amine impregnation and appendage to OMS, PSM ligand modification with amines has not yet yielded promising CO_2 adsorption properties. It is hypothesized that limited performance could result from various phenomena such as low conversion and hence low amine loading, compromised stability of the framework under the conditions required for amine grafting, low density of amines inside MOF pores, or low amine accessibility due to pore blocking.

Herein, we report a mild methodology to post-synthetically graft alkylamines to MOFs bearing amino-functionalized ligands, i.e. $Zn_4O(NH_2\text{-}BDC)_3$ (alternatively known as IRMOF-3).[19] Using a stepwise approach, the MOF was post-synthetically modified via a nucleophilic substitution between the -NH_2 groups of the ligand with BrAcBr. Next, the now pendant acetyl bromide

underwent a second reaction with selected polyamines (Scheme 1). It is noted that such a strategy has been used to post-synthetically modify the external surface of cellulose nanocrystals with different nucleophiles including amines to tailor their surface chemistry.[20] The small pore size of ~1 nm and pore volume of ~0.9 cm^3/g of $Zn_4O(NH_2\text{-}BDC)_3$ was considered when selecting the amines, which include two linear amines, ethylenediamine (ED) (~5.4 Å in length) and diethylenetriamine (DETA) (~8.0 Å in length), and a branched amine, tris(2-aminoethyl) amine (TAEA) (~4.6 Å radius). Afterwards, the extent of the modifications was quantified and the CO_2 adsorption properties of the amine-appended MOFs were assessed and compared to that of the parent material.

Materials and Methods:

All chemicals were obtained from commercial sources and used as received without further purification. Zinc nitrate hexahydrate, $Zn(NO_3)_2.6H_2O$ (Sigma Aldrich, 98 %), 2-aminoterephthalic acid, NH_2-BDC (ABCR, 98 %), bromoacetyl bromide, BrAcBr (ABCR, 98 %), tetrahydrofuran, THF (Roth, 99.5 %), N,N-dimethylformamide (DMF, 99.5 %), ethylenediamine, ED (TCI, 98 %), diethylenetriamine, DETA (TCI, 98 %), tris(2-aminoethyl)amine, TAEA (ABCR, 98 %), DMSO-d_6 (Sigma Aldrich, 99.5 % D) and DCl (ABCR, 99.5 % D).

Synthesis of $Zn_4O(NH_2\text{-}BDC)_3$: 6 g of $Zn(NO_3)_2.6H_2O$ and 1.5 g of NH_2-BDC were dissolved in 200 mL of DMF. 20 mL of reagents mixture were placed into ten 40 mL vials and heated in a preheated oven at 100 ° C for 24 h. After the reaction, the brown cubic crystals obtained were washed with 20 mL of fresh DMF three times for 1 day, and then soaked in 20 mL of fresh THF, which was exchanged three times per day for 3 days to promote solvent exchange. The $Zn_4O(NH_2\text{-}BDC)_3$ samples were kept under fresh THF for further PSM experiments, unless otherwise stated.

It should be noted that $Zn_4O(NH_2\text{-}BDC)_3$ is susceptible to collapse when dried and then exposed to air; so, the samples are kept wet for the desired PSM reactions. To obtain the weight of MOF per vials, 3 vials containing MOF samples were dried in a vacuum oven at RT for 24 h, separately. The MOF samples in each vial was then weighed and the average amount of MOF was determined to be 105 ± 5 mg/vial. Thus, for subsequent PSM reactions, 105 mg was the amount of MOF assumed in each reaction. Further, fresh $Zn_4O(NH_2\text{-}BDC)_3$ was dried under argon at RT, transferred to an adsorption cell inside a glovebox, and activated under vacuum at RT for 24 h to assess the surface area.

Synthesis of BrAc-$Zn_4O(NH_2\text{-}BDC)_3$: For the BrAcBr modification, 105 ± 5 mg of MOF was ground under THF, centrifuged, and placed in 5 mL fresh THF in a 25 mL round-bottom flask. The reaction flask was cooled in an ice-water bath (1 – 2 ^{o} C) prior to the addition of BrAcBr. Next, 39 µL (1 eq), 26 µL (0.66 eq) and 13 µL (0.33 eq) of BrAcBr (per eq of $NH_2\text{-}BDC^{2-}$ ligand in $Zn_4O(NH_2\text{-}BDC)_3$) were added dropwise to the cooled reaction mixture, and allowed to stir to RT for 24 h.

Once the reaction was complete, the product was washed three times with 10 ml of THF to remove the unreacted BrAcBr. A small fraction (~ 2.5 mg) of sample was then vacuum-dried and digested with 500 µL DMSO-*d*$_6$ and 30 µL DCl (38 wt%) to quantify the extent of conversion by ^{1}H-NMR. Further, the samples were dried under argon and activated under vacuum at RT for 24 h to assess the surface area of BrAc-$Zn_4O(NH_2\text{-}BDC)_3$. Please see the SI for details.

Synthesis of Amine-Ac-$Zn_4O(NH_2\text{-}BDC)_x$(BrAcNH-BDC)$_y$: For this step, $Zn_4O(NH_2\text{-}BDC)_3$ modified with BrAcBr, $Zn_4O(NH_2\text{-}BDC)_x(BrAcNH\text{-}BDC)_y$, was employed. By sacrificing three samples of 0.66 eq reacted $Zn_4O(NH_2\text{-}BDC)_3$, the average sample weight per vial obtained is 110 ± 1 mg. First, 110 mg of $Zn_4O(NH_2\text{-}BDC)_x(BrAcNH\text{-}BDC)_y$ was dispersed in 10 mL of fresh THF

and then cooled in an ice-water bath prior to the amine addition. Next, 18 µL ED (0.66 eq), 31 µL DETA (0.66 eq) and 44 µL TAEA (0.66 eq) were added dropwise to the reaction mixture leading to 0.66 eq ED-Ac-, 0.66 eq DETA-Ac- and 0.66 eq TAEA-Ac-$Zn_4O(NH_2\text{-}BDC)_x(BrAcNH\text{-}BDC)_y$, respectively. The reaction mixture was stirred for 24 h at RT to complete the reaction. Small amounts (~ 2.5 mg) of each sample was vacuum-dried and then digested in DMSO-d_6/DCl mixture (500/30 µL) to quantify the extent of conversion by ^{1}H-NMR analysis. Further, the samples were dried under argon atmosphere in a vial, transferred to adsorption cells inside the glovebox and then vacuum-dried at RT for 24 h prior to gas adsorption measurements.

***Synthesis of BrAc-modified Ligand**:* The BrAcBr-modified NH_2-BDC was synthesized following a previously reported procedure.[21] 3.3 g of NH_2-BDC (18.2 mmol) were dissolved in 40 mL mixture of DMF:THF (1:1) and cooled to 1-2 ^{o}C using an ice-water bath. Next, 2 mL of BrAcBr (22.9 mmol) were added dropwise to the solution and allowed to react at RT overnight. After the reaction, the resulting mixture was added to 400 mL of distilled water to precipitate out the product. The pale-yellow product was washed with copious amount of deionized water until the pH of the washings was neutral. Small amount of the product was dissolved in DMSO-d_6 and analyzed using ^{1}H-NMR to determine the purity of the obtained ligand.

Results and Discussion:

PSM-1: $Zn_4O(NH_2\text{-}BDC)_3$ with BrAcBr

$Zn_4O(NH_2\text{-}BDC)_3$ belongs to a cubic crystal system having a space group *Fm-3m*. The building blocks consist of secondary building units made of four Zn atoms connected by a µ-4 oxygen bridge (µ-4 O) forming Zn_4O building units that are further connected by ditopic amino terephthalate ligands ($NH_2\text{-}BDC^{2-}$). The MOF, $Zn_4O(NH_2\text{-}BDC)_3$, was first synthesized using previously established procedures,[22] and then underwent solvent-exchange with THF to ensure that the DMF used to make the parent MOF was completely removed from the pores. Capillary X-

ray diffraction (XRD) patterns taken of the sample in THF revealed that the as-prepared material was the desired phase and that the sample was pure (Figure 1). Nitrogen adsorption measurements, carried out at 77 K, revealed a BET surface area of 2200 m^2/g, a value that is slightly higher than the previously reported one using the same activation procedure, 1800 m^2/g.[23] Next, 0.33, 0.66, and 1 equivalents of BrAcBr per NH_2-BDC^{2-} ligand were added to the reaction flask containing $Zn_4O(NH_2\text{-}BDC)_3$, and the BrAcBr selectively acylates the pendant amino moiety of the NH_2-BDC^{2-} ligand forming an amide bond as shown in the first step of Scheme 1. This pathway is preferred as the aromatic amines are too weak to attack the electrophilic CH_2 carbon of $-CH_2Br$ moiety in BrAcBr (see NMR discussion below for details).

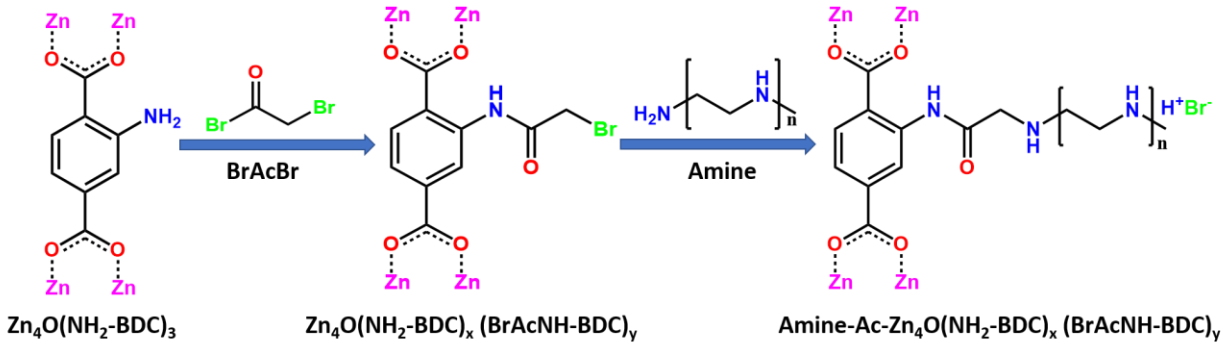

Scheme 1: Schematic of the two-step post-synthetic modification studied in this work.

After grafting the -AcBr (acetyl bromide) functionality to the MOF surface, the resulting modified MOF, $Zn_4O(NH_2\text{-}BDC)_x(BrAcNH\text{-}BDC)_y$, was sealed in a capillary for X-ray diffraction under THF (Figure 1a). Phase purity and crystallinity of the framework for each acetyl bromide loading is confirmed. Moreover, there is an increasing intensity of the diffraction peak at 6° in 2θ, which originates from the (111) plane of the unit cell. While this reflection is not systematically absent in the *Fm-3m* space group of $Zn_4O(NH_2\text{-}BDC)_3$, it has almost zero intensity in the unmodified structure. The notable intensity increase therefore indicates a modification in the unit cell contents, likely within the (111) plane. It is noted that the (111) plane of $Zn_4O(NH_2\text{-}BDC)_3$

contains the amine functionality of the NH_2-BDC^{2-} ligands. Thus, increasing the amount of the -AcBr functionality in the MOF structure could effectively add scattering density in this region of the unit cell (Figure S1). Next, the surface areas of the modified MOFs were measured. For this, the samples were dried under argon and then transferred into the glovebox, where the adsorption cells were filled with sample and later activated under vacuum at room temperature for 24 h. The surface areas decreased from 2200 m^2/g for the bare $Zn_4O(NH_2\text{-}BDC)_3$ to 1600 m^2/g, 1050 m^2/g and 485 m^2/g for the reactions containing $Zn_4O(NH_2\text{-}BDC)_3$ and 0.33, 0.66 and 1 eq-BrAcBr, respectively (Figure 1b); this indicates the introduction of increasing quantities of the -AcBr functionality in the MOF pores.

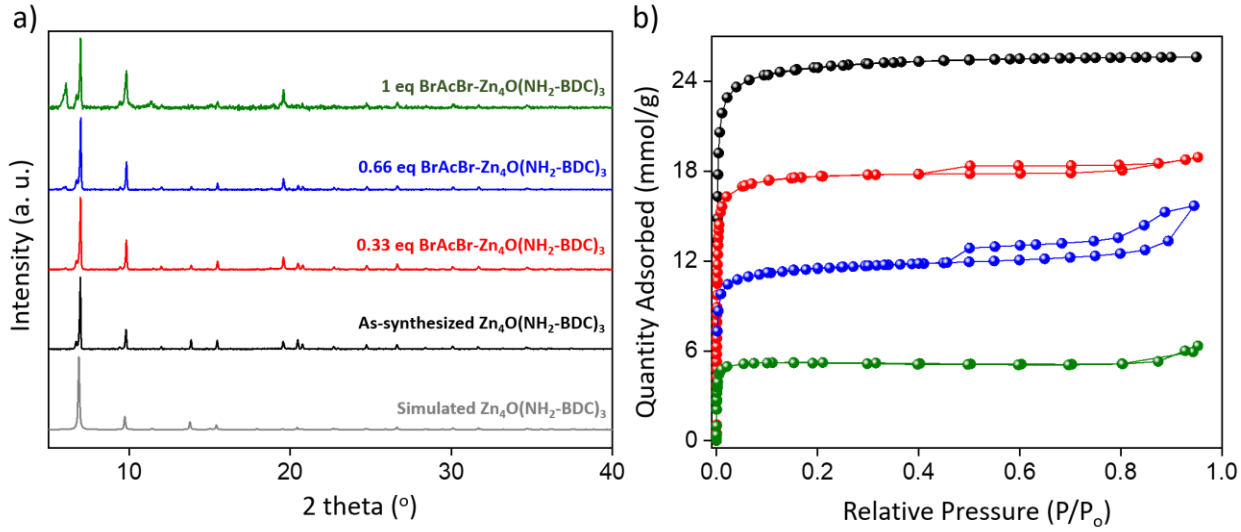

Figure 1: a) Normalized capillary X-ray diffraction patterns and b) N_2 adsorption at 77 K of the bare $Zn_4O(NH_2\text{-}BDC)_3$ (black) and 0.33 eq (red), 0.66 eq (blue) and 1 eq (olive) BrAcBr reacted $Zn_4O(NH_2\text{-}BDC)_3$, simulated diffraction pattern of $Zn_4O(NH_2\text{-}BDC)_3$ (ash).

To quantify the percentage of conversion, ^{1}H-NMR was performed on all samples, which were digested in 500 µL of DMSO-d_6 and 30 µL of DCl (38 wt%) (Figure 2). To confirm that the expected reaction occurred successfully, BrAc-modified NH_2-BDC,[21] was used as control. The

ligand was also placed under the same conditions as employed for MOF digestion; the ^{1}H-NMR signals at 8.04 ppm, 7.68 ppm, and 8.98 ppm originate from the protons on the aromatic ring and are assigned as H_d, $H_{e,}$ and H_f, respectively. The signal at 4.4 ppm originates from the two protons on the acetyl group next to the pendant Br (Figure 2v) and is assigned as H_g. For the digested samples of the modified MOF (Figures 2ii-iv), there are signals from both the modified ligand (Figure 2v, H_{d-g}) and the non-modified NH_2-BDC ligand (Figure 2i, H_{a-c}). It is noted that as the -AcBr functionalization is increased from 0.33 to 0.66 to 1 eq, the percentage of modified ligands within the $Zn_4O(NH_2\text{-}BDC)_x(BrAcNH\text{-}BDC)_y$ structure is also increased from 36 % to 60 % to 90 %, respectively. These conversion percentages are calculated from the integration values of H_e of the BrAc-NH-BDC^{2-} ligand and H_b of the non-modified NH_2-BDC^{2-} ligand in the $Zn_4O(NH_2\text{-}BDC)_3$ structure (see section S1 of the Supporting Information including the NMR characterization and Figure S2-S4). Moreover, the surface area of the -AcBr modified frameworks drops linearly with increasing conversion (Figure S5).

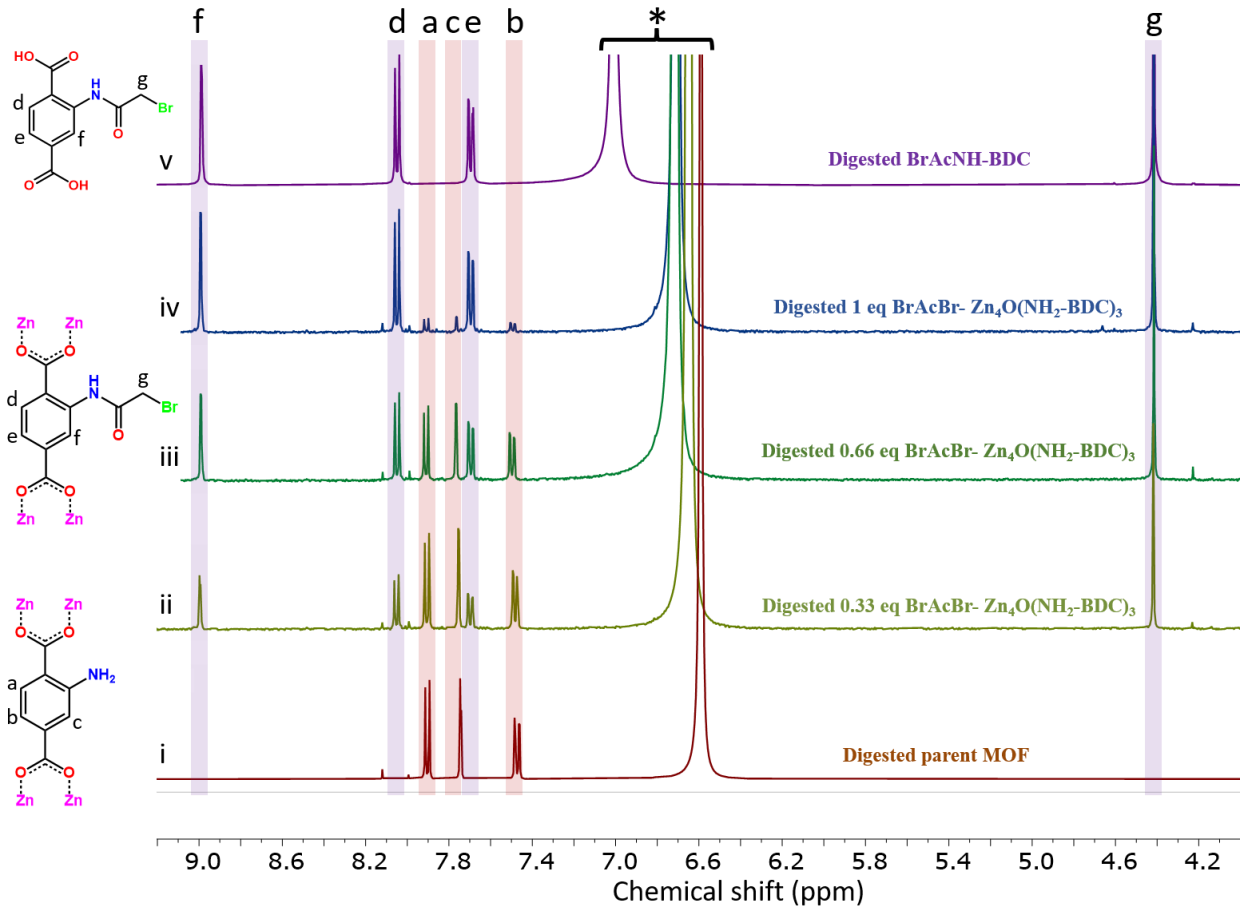

Figure 2: ^{1}H-NMR spectra of digested samples; i) $Zn_4O(NH_2\text{-}BDC)_3$, ii) 0.33 eq BrAcBr, iii) 0.66 eq BrAcBr, iv) 1 eq BrAcBr-$Zn_4O(NH_2\text{-}BDC)_3$ and v) BrAc-NH-BDC ligand (* DCl signal from 6.6 – 7.0 ppm)

PSM-2: $Zn_4O(NH_2\text{-}BDC)_x(BrAcNH\text{-}BDC)_y$ with alkylamines

Having successfully grafted -AcBr moieties into the framework, a second amine-modification step was carried out (PSM-2) with three short chain amines including ED, DETA, and TAEA. Beforehand, the stability of the parent MOF was assessed in 1 eq solutions containing each amine, and capillary X-ray diffraction patterns revealed that the structural integrity of the framework was indeed retained (Figure S6) and hence implies that PSM-2 is indeed possible. It is known that primary and secondary amines readily react with acetyl bromide moieties,[24] and thus form strong

covalent bonds between the amine and the framework. With the aim to obtain a high density of amines in the final modified structures, the framework having 90 % of ligands with the acetyl bromide modification, $Zn_4O(NH_2\text{-}BDC)_{0.3}(BrAcNH\text{-}BDC)_{2.7}$, was taken as the first candidate to test the alkylamine grafting. Unfortunately, the addition of a 1:1 ratio of amines (ED, DETA or TEAEA) to MOF ligand resulted in degradation of the ED-modified MOF structure as determined by XRD; moreover, only high angle diffraction peaks are maintained in the DETA-Ac- and TAEA-Ac- modified frameworks albeit with a very low signal to noise ratio (Figure S7). Such observations could be due to pore filling and/or the destruction of the MOF structure; the latter could stem from a decrease in stability of the -AcBr functionalized MOF to amines when compared to the parent material, $Zn_4O(NH_2\text{-}BDC)_3$. Next, ^{1}H-NMR was used to determine the percent of ligand conversion. The data showed a total conversion of ~90 %, ~30 % and ~19 % for ED-Ac-, DETA-Ac- and the TAEA-Ac- modified frameworks (Figure S8, S10-S12). Also, it is noted that a new proton signal is observed for all amine modified materials at 4.66 ppm, which could correspond to crosslinked aliphatic protons that arise from MOF ligands bridged by a single amine (Figure S8).

Next, the CO_2 adsorption properties of the materials were assessed at 313 K and compared to the parent material, $Zn_4O(NH_2\text{-}BDC)_3$. Despite the lack of crystallinity, the ED-Ac-functionalized MOF has a slight enhancement in the CO_2 capacity at low pressures, 0.15 bar, which is the pressure regime of interest for post-combustion carbon capture applications (Figure S9). Unfortunately, DETA-Ac- and TAEA-Ac-functionalized $Zn_4O(NH_2\text{-}BDC)_{0.3}(BrAcNH\text{-}BDC)_{2.7}$ displayed no enhancement in the adsorption capacity (Figure S9), an observation that could stem from the lack of accessible amines in the MOF pore. It is noted that these two materials have an incomplete conversion with large quantities of uncreated $BrAcNH\text{-}BDC^{2-}$ ligands. This means that the density

of amines inside the structure is quite low and could also imply that these amines cannot effectively diffuse into $Zn_4O(NH_2\text{-}BDC)_{0.3}(BrAcNH\text{-}BDC)_{2.7}$.

Given these aforementioned issues, the MOF having 60 % of the BrAc-modification, $Zn_4O(NH_2\text{-}BDC)_{1.2}(BrAcNH\text{-}BDC)_{1.8}$, was subsequently tested in PSM-2. It is noted that this material offers a higher surface area (1050 m^2/g) and pore volume when compared to $Zn_4O(NH_2\text{-}BDC)_{0.3}(BrAcNH\text{-}BDC)_{2.7}$; hence, it was hypothesized that this material might better allow amine diffusion, particularly for DETA and TAEA. For the reactions, 0.66 eq of each amine (including ED, DETA, or TAEA) were added to a solution containing $Zn_4O(NH_2\text{-}BDC)_{1.2}(BrAcNH\text{-}BDC)_{1.8}$. Thus, the reaction contained a 1:1 molar ratio between the modified ligand, $BrAcNH\text{-}BDC^{2-}$, and the added amine. After PSM-2, the capillary XRD patterns of the amine-modified materials imply retention of the diffraction peaks and hence, indicate that the structural integrity of the framework is maintained (Figure 3a); however, it is also noted that in this case, one cannot rule out the possible existence of an amorphous amine-containing coating on the crystalline surface of $Zn_4O(NH_2\text{-}BDC)_{1.2}(BrAcNH\text{-}BDC)_{1.8}$. Moreover, the new diffraction peak at 6 º coming from the plane (111) disappeared after PSM-2. This suggests the displacement of strongly scattering -Br from the (111) plane by the weakly scattering amines. It is noted that for the modified materials, the BET surface areas dropped drastically from 1050 m^2/g for $Zn_4O(NH_2\text{-}BDC)_{1.2}(BrAcNH\text{-}BDC)_{1.8}$ to 9 m^2/g, 69 m^2/g and 275 m^2/g for ED-Ac-, DETA-Ac- and TAEA-Ac-$Zn_4O(NH_2\text{-}BDC)_{1.2}(BrAcNH\text{-}BDC)_{1.8}$, respectively (Figure 3b). Such a drop-in surface area could arise from factors such as the framework instability, the steric effects of the amines that limit the diffusion of N_2 into the framework, or the presence of charged functionality that repel N_2.[25] Further, the pore size distribution of TAEA-Ac-$Zn_4O(NH_2\text{-}BDC)_{1.2}(BrAcNH\text{-}BDC)_{1.8}$ is found to be extended, from 0.8 – 1.7 nm, when compared to the parent $Zn_4O(NH_2\text{-}BDC)_3$ and $Zn_4O(NH_2\text{-}BDC)_{1.2}(BrAcNH\text{-}BDC)_{1.8}$, both of which have a more narrow pore size distribution of ~1.1 – 1.4 nm (Figure S13).

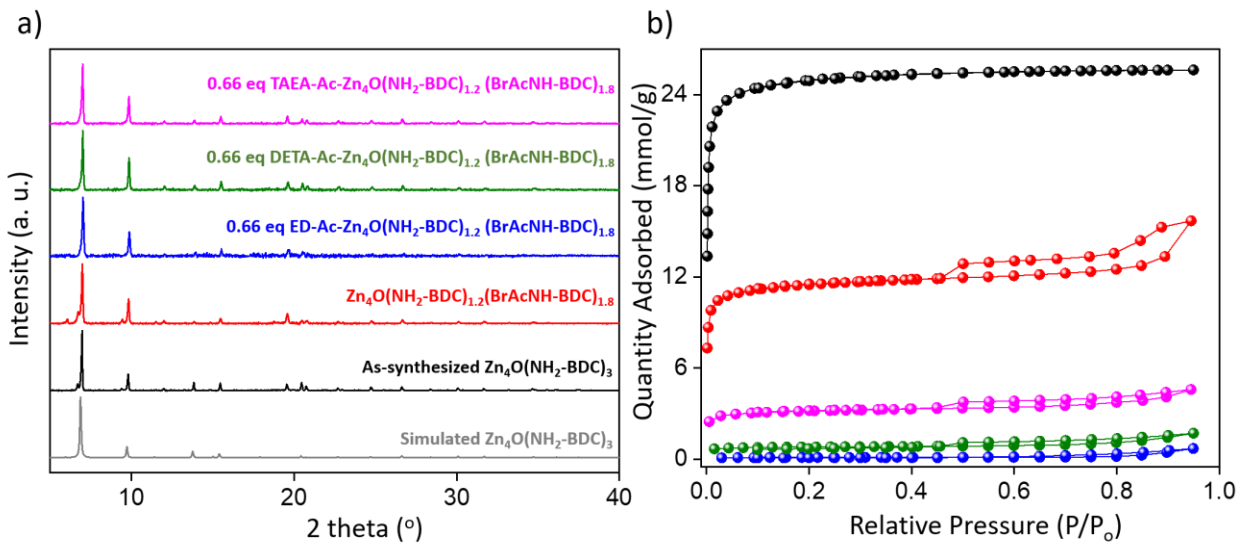

Figure 3: a) Normalized capillary X-ray diffraction patterns and b) N_2 adsorption at 77 K of bare $Zn_4O(NH_2\text{-}BDC)_3$ (black), $Zn_4O(NH_2\text{-}BDC)_{1.2}(BrAcNH\text{-}BDC)_{1.8}$ (red), ED-Ac-$Zn_4O(NH_2\text{-}BDC)_{1.2}(BrAcNH\text{-}BDC)_{1.8}$ (blue), DETA-Ac-$Zn_4O(NH_2\text{-}BDC)_{1.2}(BrAcNH\text{-}BDC)_{1.8}$ (olive) and TAEA-Ac-$Zn_4O(NH_2\text{-}BDC)_{1.2}(BrAcNH\text{-}BDC)_{1.8}$ (magenta), simulated diffraction pattern of $Zn_4O(NH_2\text{-}BDC)_3$ (ash).

Next, ^{1}H-NMR of the digested samples provided a quantitative analysis of the extent of the reaction in the three amine-modified materials (Figure 4). New signals associated with protons $H_{h\text{-}j}$ of the amine-appended moiety now appear (See Figure S14). Unfortunately, complete amine functionalization is not achieved in any case as the ^{1}H-NMR spectra include signals from three different species, including NH_2-BDC, BrAc-NH-BDC, and Amine-Ac-NH-BDC. While some of the new peaks arising from protons associated with the amine grafting step in PSM-2 ($H_{h\text{-}i}$) overlap with proton signals of BrAc-NH-BDC ($H_{d\text{-}e}$) (Figure 4 and S14), new aromatic proton signals labeled H_j are well distinguished from the equivalent signal labelled H_f of the BrAc-NH-BDC. During the substitution reactions with the amine, the -Br acts as a leaving group; so, the electron density around H_j is lowered and hence is shifted upfield in the NMR spectrum. A similar trend is

observed with the aliphatic H_g at 4.4 ppm, which is located in close proximity to the -Br of the BrAc-NH-BDC; this peak is shifted to 4.2 ppm (H_k) once the -Br is substituted with the -NH- group forming Amine-Ac-NH-BDC. In addition to these protons, the signature amine signals are observed at 3.2 - 3.1 ppm. By comparing the integration ratios of H_j at 8.8 ppm for ED-Ac-, DETA-Ac-, or TAEA-Ac-$Zn_4O(NH_2\text{-BDC})_{1.2}(BrAcNH\text{-BDC})_{1.8}$ with that of H_f at 9 ppm, the conversion percentage of BrAcNH-BDC to the aminated ligand, Amine-Ac-NH-BDC, were calculated (Section S1. NMR characterization and Figure S15-17). The calculations reveal that a total of 30 %, 28 % and 19 % of the MOF ligands were grafted with ED, DETA and TAEA, respectively. It is noted that for DETA and TAEA, the amount of amine appended to $Zn_4O(NH_2\text{-BDC})_{1.2}(BrAcNH\text{-BDC})_{1.8}$ (28% and 19 %, respectively) is similar to that achieved in $Zn_4O(NH_2\text{-BDC})_{0.3}(BrAcNH\text{-BDC})_{2.7}$ (30 % and 19 % respectively); this implies that decreasing the amount of -AcBr functionalization in the MOF did not improve the diffusion of these amines (radius 4.0 Å and ~4.6 Å respectively) into the framework. Moreover, the larger extent of conversion obtained in the reactions containing ED and DETA could be due to their linear nature and smaller radii relative to TAEA. It is noted that amines react rapidly with BrAcBr. This, combined with slow amine diffusion, might in some cases create a heterogeneous distribution, where there are more amines located on the external MOF surface. As such, using MOFs with larger pore dimensions could help facilitate better amine diffusion and hence larger quantities of amine functionalization that is also more well distributed throughout the material.

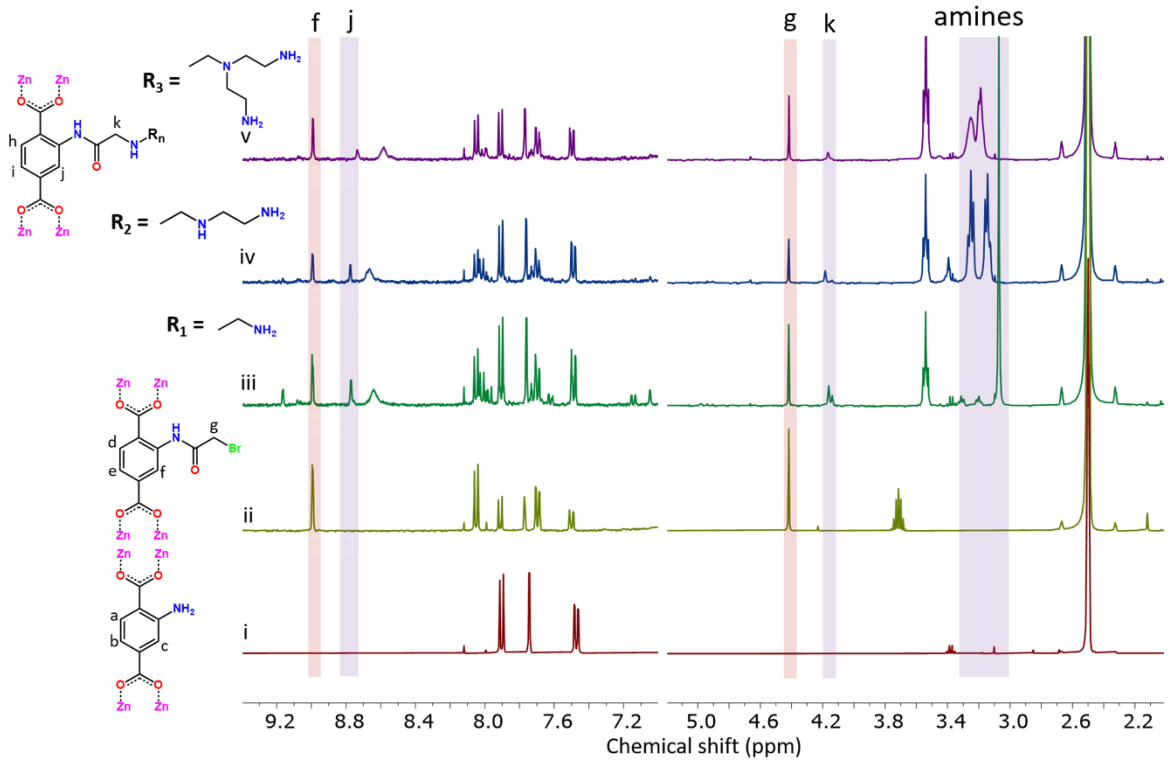

Figure 4: ^{1}H-NMR spectra of digested samples; i) $Zn_4O(NH_2\text{-}BDC)_3$, ii) $Zn_4O(NH_2\text{-}BDC)_{1.2}$ $(BrAcNH\text{-}BDC)_{1.8}$, iii) 0.66 eq ED-Ac-, iv) 0.66 eq DETA-Ac- and v) 0.66 eq TAEA-Ac-$Zn_4O(NH_2\text{-}BDC)_{1.2}$ $(BrAcNH\text{-}BDC)_{1.8}$.

Next, to compliment the NMR data, the digested amine-Ac-$Zn_4O(NH_2\text{-}BDC)_{1.2}(BrAcNH\text{-}BDC)_{1.8}$ samples were analyzed via ESI-MS. The mass spectra displayed m/z values corresponding to one amine grafted to one ligand as well as crosslinked ligands, where one amine bridges two BrAc-NH-BDC ligands (for ED-Ac- and DETA-Ac-functionalized MOF) or three BrAc-BDC ligands (for the TAEA-Ac-functionalized MOF) (Figure S18-S20). It is noted that the relative intensity of the peaks associated with the crosslinked ligands correspond to less than 10 % of the mono-grafted ligands; their low concentration could make it difficult to distinguish such peaks in the NMR. Although, it is noted that for ED-Ac-$Zn_4O(NH_2\text{-}BDC)_{1.2}(BrAcNH\text{-}BDC)_{1.8}$ an

additional signal, albeit small, is visible in the ^{1}H-NMR spectrum around 9.2 and 7.2 ppm that is still unidentified.

Thereafter, ion chromatography (IC) was employed to understand the presence of Br^- in the framework. Surprisingly, the results indicate that there are similar quantities of Br^- in $Zn_4O(NH_2\text{-}BDC)_{1.2}(BrAcNH\text{-}BDC)_{1.8}$ (7.91 wt%) and ED-Ac-, DETA-Ac- and TAEA-Ac-$Zn_4O(NH_2\text{-}BDC)_{1.2}(BrAcNH\text{-}BDC)_{1.8}$ (7.77, 7.85 and 7.78 wt% respectively). Therefore, it is hypothesized that after the S_N2 reaction with amines in the PSM-2, the Br^- remains in the amine-modified MOFs as a $[amineH]^+Br^-$ salt (Figures S21-24).

Given the presence of amine species inside the MOF pores, which can chemisorb CO_2 via a nucleophilic attack on the C atom of the CO_2 molecule,[26] the CO_2 adsorption properties of the materials were assessed at 313 K. For this, the parent MOF and amine-modified samples were dried under argon at RT for 24 h. From the data shown in Figure 5a, TAEA-Ac-$Zn_4O(NH_2\text{-}BDC)_{1.2}(BrAcNH\text{-}BDC)_{1.8}$ is the only material that showed a slight improvement in CO_2 uptake at 0.15 bar (0.16 mmol/g) when compared to the bare $Zn_4O(NH_2\text{-}BDC)_3$ (0.13 mmol/g). Unfortunately, both ED-Ac- and DETA-Ac-modified MOFs have lower CO_2 adsorption (0.12 and 0.024 mmol/g) at 0.15 bar (Figure 5a inset). It is likely that the density of amines inside the MOF pores is too low to boost in the CO_2 adsorption capacity of the amine modified materials significantly, particularly considering the presence of the aforementioned salt species in the pore that offer weaker interactions with CO_2 when compared to primary amines.[27] Despite this, it is clear that in the low pressure regime DETA-Ac- and TAEA-Ac-$Zn_4O(NH_2\text{-}BDC)_{1.2}(BrAcNH\text{-}BDC)_{1.8}$ have a steep rise in the CO_2 adsorption when compared to $Zn_4O(NH_2\text{-}BDC)_3$. This would indicate an enhanced CO_2 binding. As such, the isosteric heats of CO_2 adsorption was determine for these two materials. For this, variable temperature CO_2 adsorption data were collected at 278

K, 295 K and 313 K (Section S1 and Figure S25-S27) and the isosteric heats were extracted from the data using a dual site Langmuir model for the two amine-functionalized frameworks and a single site Langmuir model for the parent $Zn_4O(NH_2BDC)_3$ (Table S2-S4). The initial Q_{st} of TAEA-Ac-$Zn_4O(NH_2\text{-}BDC)_{1.2}(BrAcNH\text{-}BDC)_{1.8}$ is calculated to be -62.5 kJ/mol, which is within the chemisorption regime for CO_2. Moreover, the Q_{st} of DETA-Ac-$Zn_4O(NH_2\text{-}BDC)_{1.2}(BrAcNH\text{-}BDC)_{1.8}$ is -40 kJ/mol at low surface coverage, a value that is expectedly higher that the Q_{st} observed for the parent $Zn_4O(NH_2\text{-}BDC)_3$, -21 kJ/mol. The higher Q_{st} associated with the amine-grafted materials is easily explained as it is well known that CO_2 reacts with amines to form carbamate and carbamic acid species. As such, these structural features would certainly enhance the Q_{st}.[28] Further, CO_2 can form adducts with charged species, like $[amineH]^+Br^-$,[27] in the MOF pores and hence can also boost the Q_{st} relative to $Zn_4O(NH_2\text{-}BDC)_3$.

When studying materials of interest in carbon capture applications, one must also consider their selectivity for CO_2/N_2, the main components in post-combustion flue gas. In addition to amines, previous work shows that the existence various charged species inside MOF pores can aid CO_2/N_2 selectivity.[25] This stems from differences in the physical properties of these two small molecules, such as their quadrupole moment and polarizability. For N_2, these values are 15.2 x 10^{-27} esu^{-1} cm^{-1} and 17.4 x 10^{-23} cm^{-1}, respectively, while for CO_2 they are 43.0 x 10^{-27} esu^{-1} cm^{-1} and 29.1 10^{-23} cm^{-1}, respectively; therefore, charged surfaces would favor CO_2 adsorption over N_2. Moreover, it is noted that the kinetic diameter of N_2 (3.64 Å) is also larger than CO_2 (3.3 Å), and hence might further limit the diffusion of the N_2 into the amine-modified MOFs. All of these factors could play a role in the very low accessible surface areas (which are reduced by 74 to 99 %) and also boost the CO_2/N_2 selectivity of the materials. Given this, the IAST selectivity[29] for CO_2/N_2 (15/85) was determined from the CO_2 and N_2 isotherms collected at 313 K. While the

selectivity of the parent MOF is 4.1, the values obtained for DETA-Ac- and TAEA-Ac-functionalized frameworks are significantly enhanced with values of 110 and 143, respectively (Figure 5a, for values Table S1).

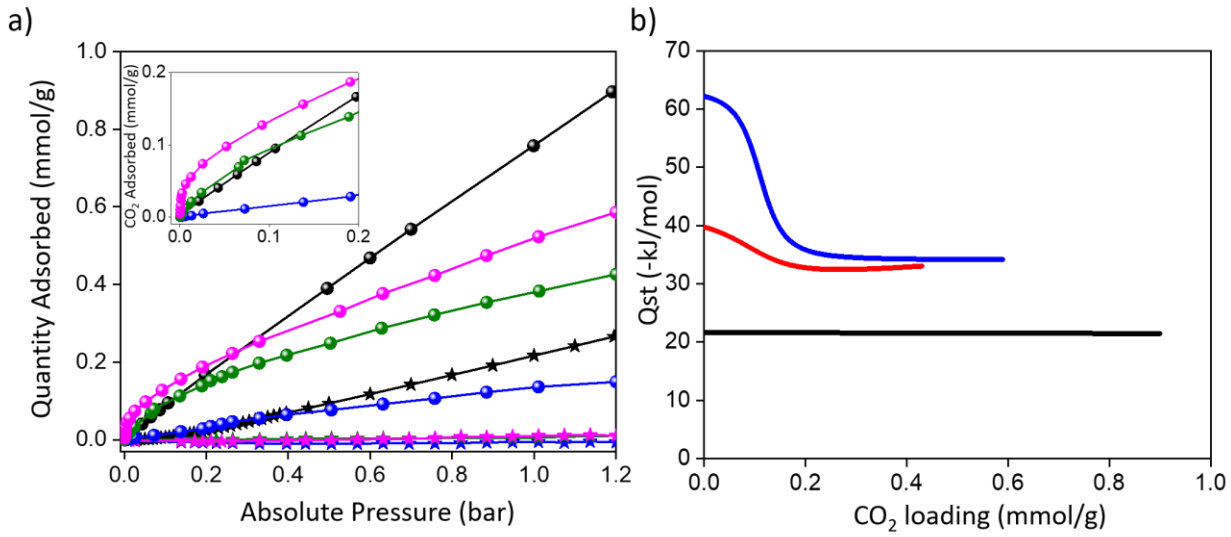

Figure 5: a) CO_2 (spheres) and N_2 (stars) adsorption isotherms at 313 K of $Zn_4O(NH_2\text{-}BDC)_3$ (black), 0.66 eq ED-Ac-$Zn_4O(NH_2\text{-}BDC)_{1.2}(BrAcNH\text{-}BDC)_{1.8}$ (blue), DETA-Ac-$Zn_4O(NH_2\text{-}BDC)_{1.2}(BrAcNH\text{-}BDC)_{1.8}$ (olive) and TAEA-Ac-$Zn_4O(NH_2\text{-}BDC)_{1.2}(BrAcNH\text{-}BDC)_{1.8}$ (magenta). The low-pressure CO_2 adsorption isotherm is presented in the inset. and b) isosteric heat of adsorption (Q_{st}) plot of $Zn_4O(NH_2\text{-}BDC)_3$ (black) DETA-Ac-$Zn_4O(NH_2\text{-}BDC)_{1.2}(BrAcNH\text{-}BDC)_{1.8}$ (red) and TAEA-Ac-$Zn_4O(NH_2\text{-}BDC)_{1.2}(BrAcNH\text{-}BDC)_{1.8}$ (blue).

Given the significant boost in the CO_2/N_2 selectivity and the isosteric heat of CO_2 adsorption, the CO_2 adsorption mechanism of TAEA-Ac-$Zn_4O(NH_2\text{-}BDC)_{1.2}(BrAcNH\text{-}BDC)_{1.8}$ was also probed via in-situ DRIFTS measurements performed at RT. For this, the modified MOF sample was mixed with KBr and evacuated at RT for 24 h prior to the measurements. The framework (mixed with KBr) was used as background collection before the CO_2 was dosed at a pressure of 1 bar. The pressure of the sample cell was subsequently reduced to a pressure of 0.2 torr, and DRIFTS

measurements were collected to highlight the vibrational modes associated with the adsorbed CO_2. It is noted that in the region where chemisorbed CO_2 is observed, between 1200 – 1800 cm^{-1}, there are many new peaks in the DRIFTS spectrum due to chemisorptive interactions between the CO_2 and amine-based moieties now grafted to the MOF wall (Figure 6). For instance, the characteristic C=O stretching mode of carbamate/carbamic acid is observed at 1715 cm^{-1} and a secondary amine N-H stretching is observed at 3444 cm^{-1} (Figure S30a). The shoulder at 1690 cm^{-1} results from a slight shift in the aforementioned C=O stretch of the carbonyl group of carbamate/carbamic acid owed to additional hydrogen bonding interactions.[30] The IR peaks for carbamates observed at 1525 cm^{-1} and 1478 cm^{-1} are attributed to asymmetric and symmetric stretching vibrations of the COO^- species bound to secondary amines and 1313 cm^{-1} is related to $NCOO^-$ skeletal vibration.[31-32] In addition, peaks at 1645 cm^{-1} and between 2750 – 1750 cm^{-1} are assigned to N-H deformation of amines and ammonium ions (NH_2^+, NH_3^+, NH^+) in response to chemisorbed CO_2 (Figure S28a).[32] Due to the polarizability of CO_2, charged species like anions (Br^-) can form adducts with CO_2. In such adducts, the negatively charged anions attack the electropositive C atom of CO_2 forming a bent configuration, denoted $CO_2^{\delta-}$, where the negative charge is now distributed around the C atom of CO_2.[27] The symmetric and asymmetric stretch (C-O) of the chemisorbed $CO_2^{\delta-}$ is observed in the range of 1210 - 1280 cm^{-1} and 1660 -1680 cm^{-1}, respectively , and the peak at 1280 cm^{-1} is assigned to the C-O stretch of $CO_2^{\delta-}$ in the presence of hydrogen bonding.[33-34] Also, in the region 3000–3500 cm^{-1} (Figure S30a), N-H stretching owed to interactions between NH····O=C (of the carbamate/carbamic acid and $CO_2^{\delta-}$) are also observed.[35-36] Also, O-H stretching influenced by interaction between OH····NH (of the carbamic acid/carbamate) is observed at 3178 cm^{-1} (Figure S30a).[37] In addition to chemisorbed species, physisorbed CO_2 can also be seen in the DRIFTS data. For instance, the linear stretching mode of the physisorbed CO_2 is observed at 2337 cm^{-1}

(Figure S28b). From the DRIFTS data, it is concluded that the observed Q_{st} of -62.5 kJ/mol for the TAEA-Ac- modified MOF (Figure 5b), which is on the lower end for chemisorbed CO_2, is likely to originate from the H-bonding interaction between chemisorbed CO_2 and basic polar amines.[30] Moreover, the modest Q_{st} value and results from the DRIFTS experiments imply that there is no formation of carbamate chains or carbamic acid pairs which often lead to higher Q_{st} values.[28] This likely stems from the fact that there is a low density of amines and that the amines are covalently grafted to the MOF wall, immobilizing them in the pores; both factors that can inhibit the formation of pairing and chains.

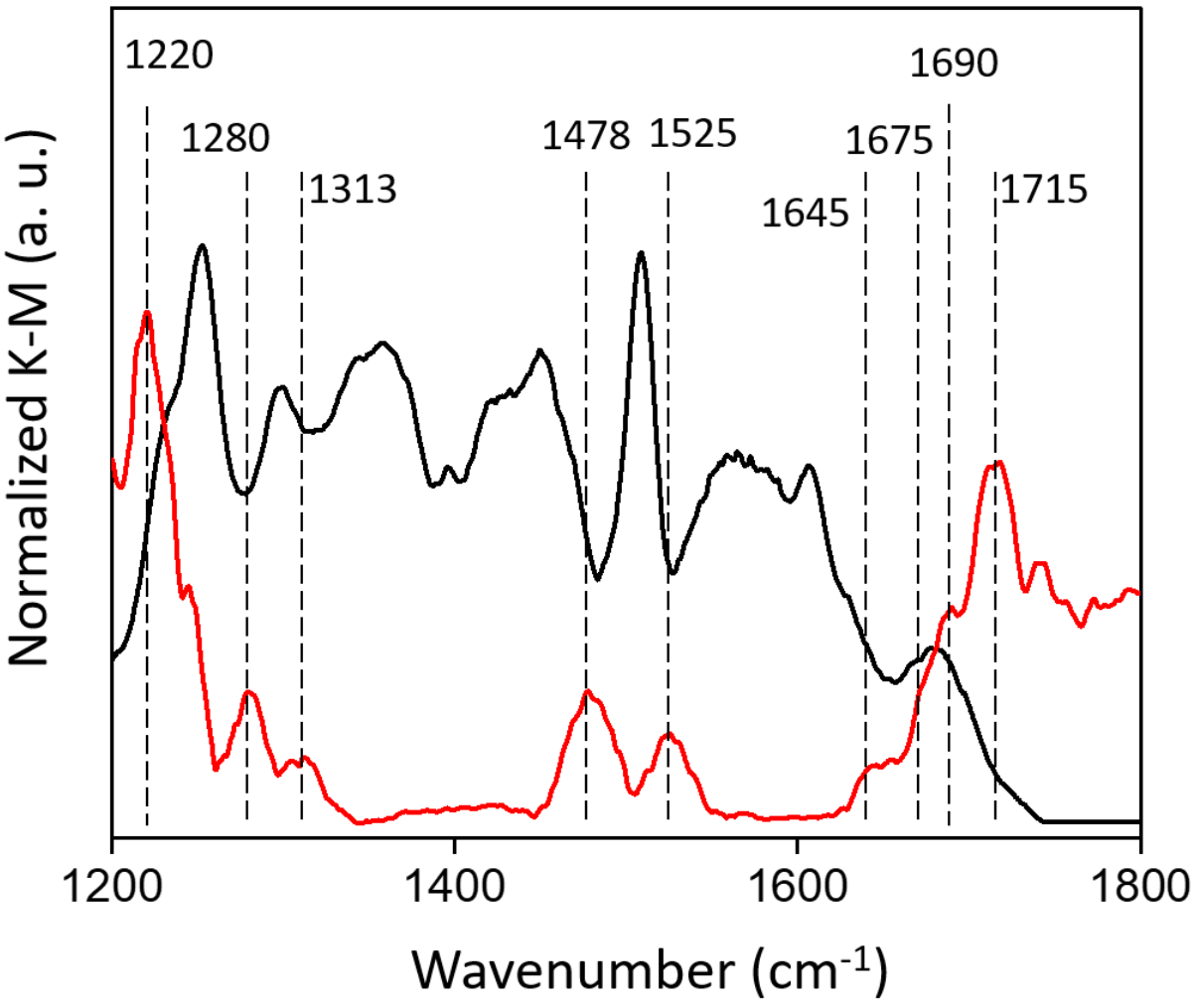

Figure 6: DRIFTS spectra of TAEA-Ac-$Zn_4O(NH_2\text{-}BDC)_{1.2}(BrAcNH\text{-}BDC)_{1.8}$ (black) with KBr subtracted as the background and CO_2-dosed TAEA-Ac-$Zn_4O(NH_2\text{-}BDC)_{1.2}(BrAcNH\text{-}BDC)_{1.8}$ (red) with the spectrum of TAEA-Ac- $Zn_4O(NH_2\text{-}BDC)_{1.2}(BrAcNH\text{-}BDC)_{1.8}$ (in KBr and without CO_2) subtracted from the background.

When comparing the DRIFTS measurements obtained from DETA-Ac- to that of TAEA-Ac-modified MOF, it is noted that the DETA-analogue displays more minor contributions from carbamate/carbamic acid, which form during the chemisorption of CO_2. Moreover, there are contributions from the more weakly chemisorbed $CO_2^{\delta-}$, physisorbed CO_2, and H-bonding interaction between the chemisorbed CO_2/$CO_2^{\delta-}$ and amines (Figure S29a-b, S30b). This data, which supports the lower observed initial Q_{st} value of -40 kJ/mol in the case of DETA, is not surprising as the TAEA has more primary amines due to a branched structure. As such, once grafted to the MOF, the TAEA is likely to present a number of primary amines despite the presence of the $[amineH]^+Br^-$ salt formed during PSM-2. However, it is expected that most of the primary amines of DETA are likely converted to the $NH_3^+Br^-$ salts during PSM-2. Such structural features would have a strong impact on the strength and nature of the CO_2 adsorption.

Last, it is noted that the Q_{st} of the physisorbed CO_2, observed at higher surface coverage in the Q_{st} plot (Figure 5b) for the DETA-Ac and TAEA-Ac functionalized MOFs is still 10-15 kJ/mol higher than the unfunctionalized $Zn_4O(NH_2\text{-}BDC)_3$; this supports the idea that there are adducts that form via interaction between CO_2 and Br^- as well as H bonding interactions between the H atoms of the amines and the O atom of the $CO_2^{\delta-}$, which are absent in the parent framework. It is noted that previous work has shown that the presence of charged species in the pores can boost the Q_{st} via electrostatic interaction.[38] Moreover, even though the strong chemisorptive interactions are blocked with the formation of $[amineH]^+Br^-$ salts, the weak chemisorption induced by these

charged species gives rise to a moderate Q_{st}, which could lend to lower regeneration energies for materials during CO_2 desorption.

Conclusion:

A new strategy to post-synthetically graft short chain polyamines into MOF pores under mild conditions is presented. This strategy combines two PSM steps. First, MOFs constructed by amine-containing ligands are reacted with BrAcBr, which is subsequently used as a bridging molecule to covalently graft alkylamines, such as ED, DETA, and TAEA, inside the MOF pores. For the proof of concept, a Zn-MOF, $Zn_4O(NH_2\text{-}BDC)_3$, was employed with the aim to characterize and quantify each PSM step, thus demonstrating the potential of this new modification strategy. In the first step (PSM-1), BrAcBr was controllably grafted into the pores of $Zn_4O(NH_2\text{-}BDC)_3$; modified materials having 36%, 60%, and 90% of acetyl bromide functionalized ligands, $Zn_4O(NH_2\text{-}BDC)_x(BrAcNH\text{-}BDC)_y$, were produced. For the second amine grafting step (PSM-2), the materials produced in PSM-1 were subsequently exposed to solutions containing ED, DETA, and TAEA. It is noted that as much as 90 % of the MOF ligands could be grafted with ED, while for DETA and TAEA, the values are much lower, approximately 30% and 19%, respectively. This is not surprising as TAEA and DETA are larger than ED, a feature which could limit the diffusion of the amines into the pores of the selected microporous Zn-MOF.

After the amine grafting, CO_2 adsorption measurements were carried out (at 313 K) on the parent and amine functionalized materials. It is noted that the CO_2 adsorption capacity of the amine-modified materials at 0.15 bar is either lower than or only slightly enhanced when compared to the parent MOF (0.13 mmol CO_2/g). This stems from the low density of amines in the MOF pores space, which is influenced by the following factors: first, IC analysis revealed that the Br^- ion concentration in the bromoacetyl bromide MOFs produced during PSM-1 is equivalent to the Br^-

ion concentration in the amine appended MOFs produced in PSM-2; this result implies that, rather than the Br^- being removed during PSM-2 (as desired), the amines are instead likely to be protonated and coordinated with Br^- counter ions forming $[amineH]^+Br^-$ salt species in the MOF pores. The formation of such salt species will inhibit the ability of the amines to strongly chemisorb the CO_2, also limiting the low-pressure adsorption. Second, the percentage of MOF ligands that can be grafted to DETA and TAEA is limited to less than 30%, also limiting the amount of CO_2 that can chemisorb in the resulting structures. Third, ESI-MS reveals that some of the MOF ligands (up to 10%) are dimerized by the bridging amines. While we were unable to determine if these dimers are formed during the PSM-2 or after the MOF digestion, such crosslinking during PSM-2 would reduce the number of primary amines in the MOF pores, again limiting the material's CO_2 capacity in the low pressure regime.

It is noted that the best performing CO_2 adsorbent, denoted TAEA-Ac-$Zn_4O(NH_2$-BDC$)_{1.2}$(BrAcNH-BDC$)_{1.8}$, contains a branched amine and hence has a higher density of primary amines (~ 19 %), when compared the linear analogues, ED and DETA. Moreover, while the CO_2 adsorption capacity (0.16 mmol CO_2/g) of TAEA-Ac-$Zn_4O(NH_2$-BDC$)_{1.2}$(BrAcNH-BDC$)_{1.8}$ is only slightly enhanced, when compared to the parent $Zn_4O(NH_2$-BDC$)_3$ (0.13 mmol CO_2/g) at 0.15 bar, the IAST CO_2/N_2 (15/85) selectivity is found to be ~ 35 times higher than the parent MOF. Further, the isosteric heat of CO_2 adsorption, determined from variable temperature adsorption isotherms, is -62.5 kJ/mol for TAEA-Ac-$Zn_4O(NH_2$-BDC$)_{1.2}$(BrAcNH-BDC$)_{1.8}$, a value that is almost three times that observed for the parent framework. Finally, the CO_2 adsorption mechanism of TAEA-Ac-$Zn_4O(NH_2$-BDC$)_{1.2}$(BrAcNH-BDC$)_{1.8}$ was probed by in-situ DRIFTS measurements, and the study indicates a combination of several different types of interactions

including both the chemisorption and physisorption of CO_2 as well as H-bonding interactions with species formed during the chemisorption of CO_2.

While the CO_2 adsorption capacities and the material's stability in humid environments (Figure S31) are not yet in a regime that is compatible for practical post-combustion carbon capture applications, the enhancement in the isosteric heat and CO_2/N_2 selectivity, achieved with the new PSM strategy, is promising. It is envisioned that applying the same chemistry to other more robust MOFs with varying structures and higher pore volumes is an approach to optimize the CO_2 uptakes in the low pressure regime; such work could eventually lead to the design of new, alternative capture systems that can contribute to reducing global CO_2 emissions.

ASSOCIATED CONTENT

Supporting Information. Description of the characterization tools and calculation methods, capillary XRD spectra, ^{1}H-NMR spectra, ESI-MS spectra, IC spectra, CO_2 and N_2 adsorption isotherms and fittings, in situ DRIFTS spectra.

The following files are available free of charge.

The file is available in PDF format.

AUTHOR INFORMATION

Corresponding Author

*Wendy L. Queen − Institute of Chemical Sciences and Engineering, École Polytechnique Fedérale de Lausanne (EPFL), CH-1951 Sion, Switzerland

orcid.org/0000-0002-8375- 2341

Email: wendy.queen@epfl.ch.

Author Contributions

The manuscript was written through contributions of all authors. All authors have given approval to the final version of the manuscript.

Funding Sources

This work was supported by the Swiss National Science Foundation (SNSF) under grant PYAPP2_160581

ACKNOWLEDGMENT

We thank the canton of Valais for the support of M.A and GAZNAT for J. E. We thank Dr. Natalia Gosilova for her help with ESI-MS measurement. We thank the semester student Doriane Meyer for the help.

ABBREVIATIONS

MOF, Metal Organic-Framework; ED, Ethylenediamine; DETA, Diethylenetriamine, TAEA, tris(2-aminoethyl) amine, XRD, X-ray diffraction, BrAcBr, Bromoacetyl bromide; NH_2-BDC, 2-aminoterephthalic acid; NMR, Nuclear Magnetic Resonance; IC, Ion Chromatography; ESI-MS, Electron Spray Ionization – Mass spectrometry; DRIFTS, Diffuse Reflectance Infrared Fourier Transform Spectroscopy.

REFERENCES

1. Furukawa, H.; Cordova, K. E.; O'Keeffe, M.; Yaghi, O. M., The Chemistry and Applications of Metal-Organic Frameworks. *Science* **2013,** *341* (6149), 1230444.
2. Li, H.; Li, L.; Lin, R.-B.; Zhou, W.; Zhang, Z.; Xiang, S.; Chen, B., Porous metal-organic frameworks for gas storage and separation: Status and challenges. *EnergyChem* **2019,** *1* (1), 100006.

3. Sumida, K.; Rogow, D. L.; Mason, J. A.; McDonald, T. M.; Bloch, E. D.; Herm, Z. R.; Bae, T.-H.; Long, J. R., Carbon Dioxide Capture in Metal–Organic Frameworks. *Chemical Reviews* **2012,** *112* (2), 724-781.
4. Ding, M.; Flaig, R. W.; Jiang, H.-L.; Yaghi, O. M., Carbon capture and conversion using metal–organic frameworks and MOF-based materials. *Chemical Society Reviews* **2019,** *48* (10), 2783-2828.
5. Yang, D.; Gates, B. C., Catalysis by Metal Organic Frameworks: Perspective and Suggestions for Future Research. *ACS Catalysis* **2019,** *9* (3), 1779-1798.
6. Fang, Y.; Zhang, L.; Zhao, Q.; Wang, X.; Jia, X., Application of acid-promoted UiO-66-NH2 MOFs in the treatment of wastewater containing methylene blue. *Chemical Papers* **2019,** *73* (6), 1401-1411.
7. Shi, Z.; Tao, Y.; Wu, J.; Zhang, C.; He, H.; Long, L.; Lee, Y.; Li, T.; Zhang, Y.-B., Robust Metal–Triazolate Frameworks for CO2 Capture from Flue Gas. *Journal of the American Chemical Society* **2020,** *142* (6), 2750-2754.
8. Flaig, R. W.; Osborn Popp, T. M.; Fracaroli, A. M.; Kapustin, E. A.; Kalmutzki, M. J.; Altamimi, R. M.; Fathieh, F.; Reimer, J. A.; Yaghi, O. M., The Chemistry of CO2 Capture in an Amine-Functionalized Metal–Organic Framework under Dry and Humid Conditions. *Journal of the American Chemical Society* **2017,** *139* (35), 12125-12128.
9. Asgari, M.; Jawahery, S.; Bloch, E. D.; Hudson, M. R.; Flacau, R.; Vlaisavljevich, B.; Long, J. R.; Brown, C. M.; Queen, W. L., An experimental and computational study of CO2 adsorption in the sodalite-type M-BTT (M = Cr, Mn, Fe, Cu) metal–organic frameworks featuring open metal sites. *Chemical Science* **2018,** *9* (20), 4579-4588.
10. Siegelman, R. L.; McDonald, T. M.; Gonzalez, M. I.; Martell, J. D.; Milner, P. J.; Mason, J. A.; Berger, A. H.; Bhown, A. S.; Long, J. R., Controlling Cooperative CO2 Adsorption in Diamine-Appended Mg2(dobpdc) Metal–Organic Frameworks. *Journal of the American Chemical Society* **2017,** *139* (30), 10526-10538.
11. Zhong, R.; Yu, X.; Meng, W.; Liu, J.; Zhi, C.; Zou, R., Amine-Grafted MIL-101(Cr) via Double-Solvent Incorporation for Synergistic Enhancement of CO2 Uptake and Selectivity. *ACS Sustainable Chemistry & Engineering* **2018,** *6* (12), 16493-16502.
12. Kim, E. J.; Siegelman, R. L.; Jiang, H. Z. H.; Forse, A. C.; Lee, J.-H.; Martell, J. D.; Milner, P. J.; Falkowski, J. M.; Neaton, J. B.; Reimer, J. A.; Weston, S. C.; Long, J. R., Cooperative carbon capture and steam regeneration with tetraamine-appended metal–organic frameworks. *Science* **2020,** *369* (6502), 392.
13. Lin, Y.; Yan, Q.; Kong, C.; Chen, L., Polyethyleneimine Incorporated Metal-Organic Frameworks Adsorbent for Highly Selective CO2 Capture. *Scientific Reports* **2013,** *3* (1), 1859.
14. Kang, J. H.; Yoon, T.-U.; Kim, S.-Y.; Kim, M.-B.; Kim, H.-J.; Yang, H.-C.; Bae, Y.-S., Extraordinarily selective adsorption of CO2 over N2 in a polyethyleneimine-impregnated NU-1000 material. *Microporous and Mesoporous Materials* **2019,** *281*, 84-91.
15. Peh, S. B.; Zhao, D., Tying amines down for stable CO₂ capture. *Science* **2020,** *369* (6502), 372.
16. Britt, D.; Lee, C.; Uribe-Romo, F. J.; Furukawa, H.; Yaghi, O. M., Ring-Opening Reactions within Porous Metal−Organic Frameworks. *Inorganic Chemistry* **2010,** *49* (14), 6387-6389.
17. Molavi, H.; Joukani, F. A.; Shojaei, A., Ethylenediamine Grafting to Functionalized NH2–UiO-66 Using Green Aza-Michael Addition Reaction to Improve CO2/CH4 Adsorption Selectivity. *Industrial & Engineering Chemistry Research* **2018,** *57* (20), 7030-7039.

18. Zhu, J.; Wu, L.; Bu, Z.; Jie, S.; Li, B.-G., Polyethyleneimine-Modified UiO-66-NH2(Zr) Metal–Organic Frameworks: Preparation and Enhanced CO2 Selective Adsorption. *ACS Omega* **2019,** *4* (2), 3188-3197.
19. Eddaoudi, M.; Kim, J.; Rosi, N.; Vodak, D.; Wachter, J.; Keeffe, M.; Yaghi, O. M., Systematic Design of Pore Size and Functionality in Isoreticular MOFs and Their Application in Methane Storage. *Science* **2002,** *295* (5554), 469.
20. Bullard, K. K.; Srinivasarao, M.; Gutekunst, W. R., Modification of cellulose nanocrystal surface chemistry with diverse nucleophiles for materials integration. *Journal of Materials Chemistry A* **2020,** *8* (35), 18024-18031.
21. Liu, S.; Zhai, L.; Li, C.; Li, Y.; Guo, X.; Zhao, Y.; Wu, C., Exploring and Exploiting Dynamic Noncovalent Chemistry for Effective Surface Modification of Nanoscale Metal–Organic Frameworks. *ACS Applied Materials & Interfaces* **2014,** *6* (8), 5404-5412.
22. Espín, J.; Garzón-Tovar, L.; Carné-Sánchez, A.; Imaz, I.; Maspoch, D., Photothermal Activation of Metal–Organic Frameworks Using a UV–Vis Light Source. *ACS Applied Materials & Interfaces* **2018,** *10* (11), 9555-9562.
23. Nelson, A. P.; Farha, O. K.; Mulfort, K. L.; Hupp, J. T., Supercritical Processing as a Route to High Internal Surface Areas and Permanent Microporosity in Metal−Organic Framework Materials. *Journal of the American Chemical Society* **2009,** *131* (2), 458-460.
24. Roose, P.; Eller, K.; Henkes, E.; Rossbacher, R.; Höke, H., Amines, Aliphatic. *Ullmann's Encyclopedia of Industrial Chemistry* **2015**, 1-55.
25. Kochetygov, I.; Bulut, S.; Asgari, M.; Queen, W. L., Selective CO2 adsorption by a new metal–organic framework: synergy between open metal sites and a charged imidazolinium backbone. *Dalton Transactions* **2018,** *47* (31), 10527-10535.
26. D'Alessandro, D. M.; Smit, B.; Long, J. R., Carbon Dioxide Capture: Prospects for New Materials. *Angewandte Chemie International Edition* **2010,** *49* (35), 6058-6082.
27. Quattrociocchi, D. G. S.; de Oliveira, A. R.; Carneiro, J. W. d. M.; Rocha, C. M. R.; Varandas, A. J. C., MP2 versus density functional theory calculations in CO2-sequestration reactions with anions: Basis set extrapolation and solvent effects. *International Journal of Quantum Chemistry* **2021,** *121* (8), e26583.
28. Forse, A. C.; Milner, P. J., New chemistry for enhanced carbon capture: beyond ammonium carbamates. *Chemical Science* **2021,** *12* (2), 508-516.
29. Simon, C. M.; Smit, B.; Haranczyk, M., pyIAST: Ideal adsorbed solution theory (IAST) Python package. *Computer Physics Communications* **2016,** *200*, 364-380.
30. Thirion, D.; Rozyyev, V.; Park, J.; Byun, J.; Jung, Y.; Atilhan, M.; Yavuz, C. T., Observation of the wrapping mechanism in amine carbon dioxide molecular interactions on heterogeneous sorbents. *Physical Chemistry Chemical Physics* **2016,** *18* (21), 14177-14181.
31. Richner, G.; Puxty, G., Assessing the Chemical Speciation during CO2 Absorption by Aqueous Amines Using in Situ FTIR. *Industrial & Engineering Chemistry Research* **2012,** *51* (44), 14317-14324.
32. Wilfong, W. C.; Srikanth, C. S.; Chuang, S. S. C., In Situ ATR and DRIFTS Studies of the Nature of Adsorbed CO2 on Tetraethylenepentamine Films. *ACS Applied Materials & Interfaces* **2014,** *6* (16), 13617-13626.
33. Toda, Y.; Hirayama, H.; Kuganathan, N.; Torrisi, A.; Sushko, P. V.; Hosono, H., Activation and splitting of carbon dioxide on the surface of an inorganic electride material. *Nature Communications* **2013,** *4* (1), 2378.

34. Herburger, A.; Ončák, M.; Siu, C.-K.; Demissie, E. G.; Heller, J.; Tang, W. K.; Beyer, M. K., Infrared Spectroscopy of Size-Selected Hydrated Carbon Dioxide Radical Anions CO2.−(H2O)n (n=2–61) in the C−O Stretch Region. *Chemistry – A European Journal* **2019,** *25* (43), 10165-10171.
35. Martinez-Felipe, A.; Brebner, F.; Zaton, D.; Concellon, A.; Ahmadi, S.; Piñol, M.; Oriol, L., Molecular Recognition via Hydrogen Bonding in Supramolecular Complexes: A Fourier Transform Infrared Spectroscopy Study. *Molecules* **2018,** *23* (9).
36. Andrei, H.-S.; Nizkorodov, S. A.; Dopfer, O., IR Spectra of Protonated Carbonic Acid and Its Isomeric H3O+·CO2 Complex. *Angewandte Chemie International Edition* **2007,** *46* (25), 4754-4756.
37. Srikanth, C. S.; Chuang, S. S. C., Infrared Study of Strongly and Weakly Adsorbed CO2 on Fresh and Oxidatively Degraded Amine Sorbents. *The Journal of Physical Chemistry C* **2013,** *117* (18), 9196-9205.
38. Nugent, P.; Belmabkhout, Y.; Burd, S. D.; Cairns, A. J.; Luebke, R.; Forrest, K.; Pham, T.; Ma, S.; Space, B.; Wojtas, L.; Eddaoudi, M.; Zaworotko, M. J., Porous materials with optimal adsorption thermodynamics and kinetics for CO2 separation. *Nature* **2013,** *495* (7439), 80-84.
39. Das, S.; Ghosh, C.; Jana, S., Moisture induced isotopic carbon dioxide trapping from ambient air. *Journal of Materials Chemistry A* **2016,** *4* (20), 7632-7640.

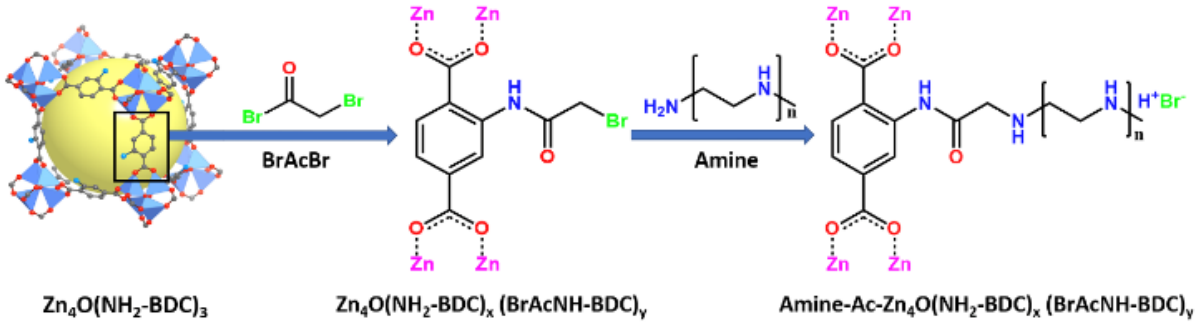

Amines are covalently grafted to the $Zn_4O(NH_2\text{-}BDC)_3$ (IRMOF-3) framework via a new, two-step post-synthetic modification strategy. The feasibility of the reaction is proved and the conversion in each step is quantitatively assessed via ^{1}H-NMR. The CO_2 adsorption performance in the post-combustion capture regime, CO_2/N_2 selectivity, isosteric heat of CO_2 adsorption and adsorption mechanism are studied.